

Supplement of

Hind- and forecasting of regional methane from coal mine emissions in the Upper Silesian Coal Basin using the on-line nested global regional chemistry climate model MECO(n)(MESSy v2.53)

Nickl et al.

Correspondance to: anna-leah.nickl@dlr.de

S1 Point Sources PCH4 emissions inventory

see the attached ascii file for details on the coal mines and single shafts, their exact locations, methane emissions and the corresponding references.

S2 Vertical profile of simulated CH4_FX and J1 and J2

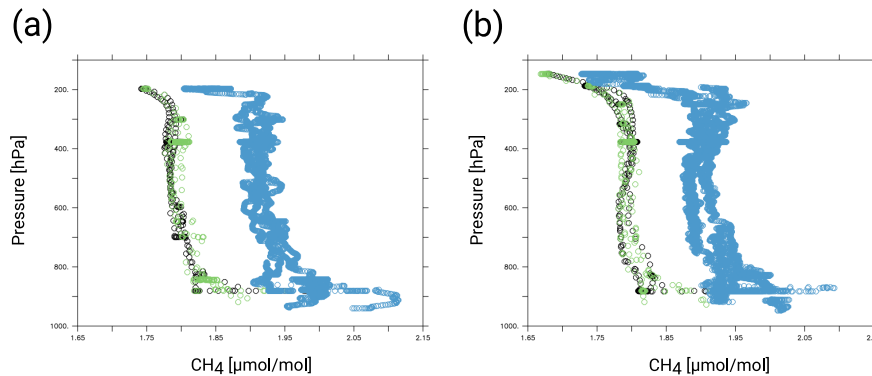


Fig. S1: Methane mixing ratios of J1 (a) and J2 (b) versus pressure (in hPa) along the flight track. Simulated CH4_FX is displayed by the green and black circles for CM7 and CM2.8, respectively. Observations are in blue.

S3 Comparisons of P1, P3, P6 and P7 to the simulated CH4_FX of CM7 and CM2.8

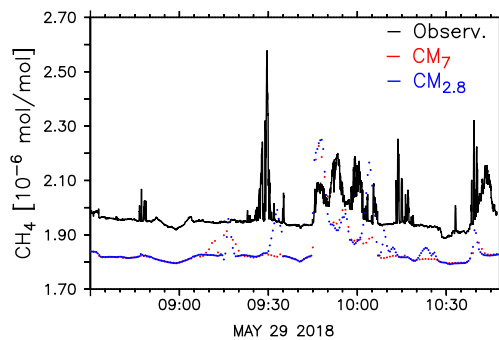


Fig. S2: Methane mixing ratios of P1 on May 29, 2018. Observations are in black, model results of CM7 and CM2.8 are in red and blue, respectively.

At 09:30 UTC D-FDLR flew close to the ventilation shafts resulting in high observed methane mixing ratios. This peak is only resolved by CM2.8, even though it is shifted in time or in space. The model performance decreases if the

measurements are taken very close to the ventilation shafts. This is also seen for P2 and P3, where localized methane enhancements cannot be resolved by the model. Between 09:45 and 10:10 UTC, the observed methane enhancements are simulated in both model instances, but show very high amplitudes compared to the observations.

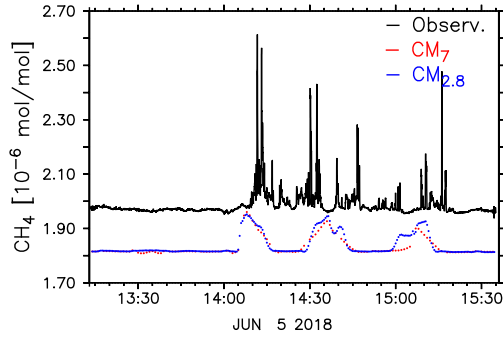


Fig. S3: Methane mixing ratios of P3 on June 05, 2018. Observations are in black, model results of CM7 and CM2.8 are in red and blue, respectively.

The comparison between D-FDLR in-situ observations and the model results show that the observed peaks can be simulated, but observations show more variability and the simulated methane peaks are shifted in time or in space, which results in a low correlation in the Taylor diagram (see Fig. 13). When catching the methane plume, the aircraft flew very close to the ventilation shafts, which resulted in high mixing ratios up to $2.65 \cdot 10^{-6}$ mol/mol. Although in general, simulated peak amplitudes and observed peak amplitudes are in good agreement, the model is not able to resolve these short-term enhancements (see also Figure S2).

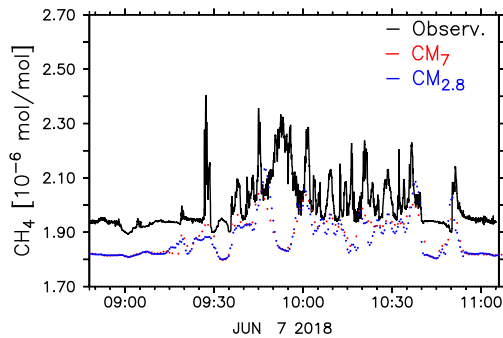


Fig. S4: Methane mixing ratios of P5 on June 07, 2018. Observations are in black, model results of CM7 and CM2.8 are in red and blue, respectively.

On June 07, model results agree well with the observed methane peaks. Besides the enhancement at 09:30 UTC, amplitudes are very similar to those of the observations. This can be also seen in the Taylor diagram (see Fig. 13), where P6 is close to the red reference line. Between 09:50 UTC and 10:00 UTC, D-FDLR flew close to the beginning of the Sudetes, right behind the Czech boarder. In concurrency with increased methane mixing ratios, high mixing ratios of CO and CO₂ have been observed here as well. These gases might have accumulated north east of the mountain range, but the model is not able to simulate this feature.

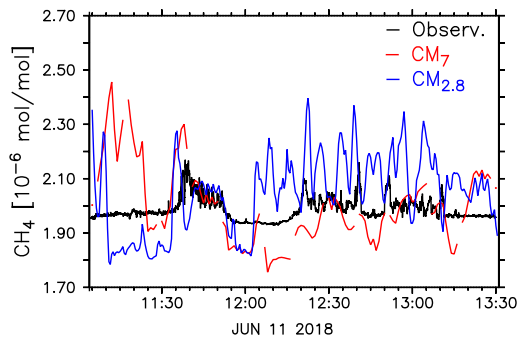


Fig. S5: Methane mixing ratios of P7 on June 11, 2018. Observations are in black, model results of CM7 and CM2.8 are in red and blue, respectively.

On June 11 wind blew predominantly from north west and the observed peak around 11:40 UTC can be attributed to the southwestern USCB mines. After 12:20 UTC, D-FDLR flew downwind of the northern USCB mines. Both model instances are able to simulate the first methane peak around 11:40 UTC, but differ from the observations before and after that peak. The model shows very high amplitudes and high variability in methane mixing ratios. High wind speeds might be the reason. The correlation coefficients of both instances are below 0.3 and the normalized standard deviation are 3.5 and 3.6 for CM2.8 and CM12, respectively. Consequently P7 lies outside the Taylor diagram in Fig.13.